

# Optical imaging of resonant electrical carrier injection into individual quantum dots

A. Baumgartner,<sup>1,\*</sup> E. Stock,<sup>2</sup> A. Patané,<sup>1</sup> L. Eaves,<sup>1</sup> M. Henini,<sup>1</sup> and D. Bimberg<sup>2</sup>

<sup>1</sup> *School of Physics and Astronomy, University of Nottingham, Nottingham NG7 2RD, UK*

<sup>2</sup> *Technical University Berlin, Hardenbergstrasse 36, 10623 Berlin, D*

(Dated: July 19, 2010)

We image the micro-electroluminescence (EL) spectra of self-assembled InAs quantum dots (QDs) embedded in the intrinsic region of a GaAs *p-i-n* diode and demonstrate optical detection of resonant carrier injection into a single QD. Resonant tunneling of electrons and holes into the QDs at bias voltages below the flat-band condition leads to sharp EL lines characteristic of individual QDs, accompanied by a spatial fragmentation of the surface EL emission into small and discrete light-emitting areas, each with its own spectral fingerprint and Stark shift. We explain this behavior in terms of Coulomb interaction effects and the selective excitation of a small number of QDs within the ensemble due to preferential resonant tunneling paths for carriers.

PACS numbers: 73.21.La, 73.63.Hs, 78.60.Fi, 78.67.Hc

Self-assembled InAs quantum dots (QDs) are an important model system for investigating the fundamental physics of quantum-confined electrons [1–3]. The selective light emission from a small number of QDs can be achieved, for example, by lithographically defined small-area diodes [4] or apertures [5], or by the incorporation of QDs into microcavities [6, 7] and nanowires [8, 9]. Such studies have provided information about the electronic properties of the dots and form the basis for novel applications, e.g. optically [10] and electrically [11] driven sources of entangled photon pairs for quantum information processing. Of particular interest is the possibility of generating sharp EL emission lines from individual QDs by voltage controlled electrical injection of carriers. Despite many works on resonant tunneling injection of carriers in unipolar QD devices [12–15], the simultaneous resonant injection of both electrons and holes required for EL emission from an individual QD has received less attention [16, 17] and is relevant to topical research on electrically driven single QD photon emitters [11].

Here we use micro-electroluminescence ( $\mu$ EL) spectroscopy and imaging to investigate the optical emission from a single layer of self-assembled InAs quantum dots embedded in the intrinsic region of a *p-i-n* light emitting diode. By gradually decreasing the applied bias below the ‘flat band’ threshold voltage at which the bias balances the built-in potential in the *i*-region, we follow the evolution of the EL spectra and the corresponding spatial form of the EL emission. We show that resonant tunneling of electrons and holes into the QDs at bias voltages below the flat band condition leads to sharp EL lines which are characteristic of individual QDs, accompanied by a spatial fragmentation of the diode emission into small and discrete light-emitting areas, each with its own spectral fingerprint and Stark shift. We explain this behavior in terms of the selective excitation of a small number of QDs within the ensemble due to the presence of preferential resonant tunneling paths for carriers. We

also discuss the effect of QD charging and Coulomb interactions on the resonant excitation of the single QD EL emission. This demonstration of bias-controlled excitation of EL from an individual QD within an ensemble of dots could be developed further for use in optoelectronic or quantum information applications.

Our *p-i-n* diodes were grown by molecular beam epitaxy on a  $p^+$  GaAs substrate, which forms the bottom electrical contact of the diode. The layer structure in order of growth on the substrate is as follows: 200 nm and 50 nm *p*-doped GaAs layer with  $p = 4 \times 10^{18} \text{ cm}^{-3}$  and  $p = 5 \times 10^{17} \text{ cm}^{-3}$ , respectively; a 6 nm intrinsic GaAs spacer layer; a 1.8 monolayer (ML) of InAs, which gives rise to a wetting layer (WL) and QDs with a density of about  $10^{10} \text{ cm}^{-2}$ . The QD layer is covered by 16 nm of intrinsic GaAs followed by 50 nm *n*-doped GaAs ( $n = 2 \times 10^{16} \text{ cm}^{-3}$ ) and a 500 nm GaAs top layer with  $n = 4 \times 10^{18} \text{ cm}^{-3}$ . The diodes are defined by wet-chemical etching and a ring-shaped gold electrode forms the top electrical contact and provides optical access. Here we focus on large area devices with 200  $\mu\text{m}$  diameter, containing  $\sim 10^6$  QDs. A schematic band diagram for a bias  $U$  below the flat band condition, i.e. for  $U < 1.5 \text{ V}$ , is shown in the inset of Fig. 1a. The  $\mu$ EL spectra were recorded at  $T \approx 15 \text{ K}$  with a spectral resolution of  $\sim 40 \mu\text{eV}$  and a focal spot diameter of about 20  $\mu\text{m}$ . The spatial maps of the  $\mu$ EL were recorded by scanning the focusing mirror along the mesa.

Figure 1(a) shows the EL spectra for a range of applied biases  $U$ . As  $U$  is decreased below the flat band condition, the EL spectrum narrows and evolves into single sharp EL lines. To track the evolution of the EL spectrum with  $U$ , we show in Fig. 1(b) a color-scale plot of the normalized EL intensity versus  $U$  and the photon energy,  $h\nu$ . This reveals clearly the narrowing of the QD emission with decreasing bias and the emergence of two distinct EL features, labeled A and B and indicated in Fig. 1b by dashed lines. A and B both shift to lower en-

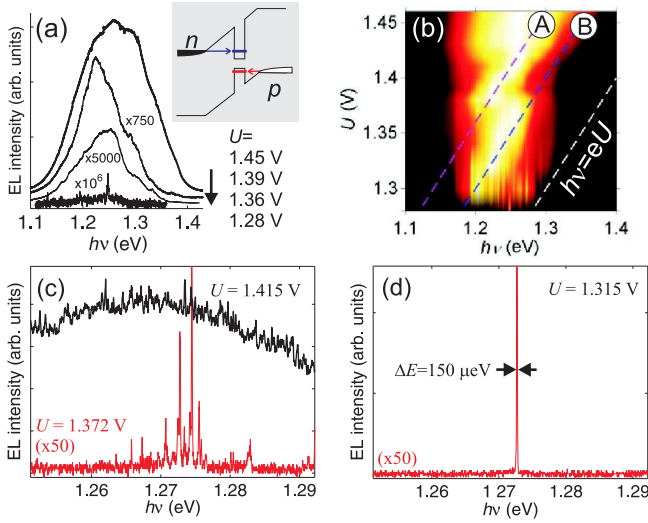


FIG. 1: (Color online) (a) EL spectra of the diode for a series of bias voltages  $U$ . Inset: schematic diagram of the resonant injection of electrons and holes into a QD. (b) Colorscale image of the normalized EL intensity as a function of photon energy and bias. The dashed lines represent the conditions  $eU = h\nu$ ,  $eU = h\nu + 100$  meV and  $eU = h\nu + 160$  meV. (c) and (d)  $\mu$ EL spectra showing the fragmentation of the continuous EL spectrum into a sharp emission line.

ergies with decreasing bias with peak energies that run parallel to the line  $eU = h\nu$ . The energy difference between the excitation energy  $eU$  and the peak energy of each feature is  $E_A = 160$  meV and  $E_B = 100$  meV, respectively. This indicates that electron-hole pairs electrically injected into different QDs relax approximatively the same energy prior to the radiative recombination in the ground state.

We now focus on the  $\mu$ EL spectra in the energy interval  $1.25$  eV  $< h\nu < 1.29$  eV at low applied bias. Figure 1c and 1d show the  $\mu$ EL spectrum at a given position on the mesa at different  $U$ . With decreasing  $U$  the spectrum evolves from a broad continuous emission into a fragmented spectrum. At  $U = 1.315$  V the emission consists of a single sharp line only, with a full width at half maximum of  $\sim 150$   $\mu$ eV. This linewidth is not determined by the resolution of the spectrometer and is similar to the typical linewidths reported for the low temperature photoluminescence emission of individual InAs QDs [18]. This method of EL excitation allows the study of such sharp emission lines over several orders of magnitudes in intensity and also reveals a characteristic exponential acoustic phonon broadening and a weak but sharp phonon replica peak, which are reported elsewhere [19].

The fragmentation of the EL spectrum into sharp lines is accompanied by a spatial fragmentation of the EL emission. To demonstrate this effect, we recorded  $\mu$ EL spectra at each position of a square grid covering roughly 1/4 of the diode surface. Figure 2 shows spatial maps of the maximum intensity of each spectrum as a function of

position for a series of bias voltages. For each image, a scale factor relates the maximum of the colorscale to the maximum at  $U = 1.415$  V.

At  $U = 1.415$  V the emission is essentially homogeneous across the scan [20]. At a slightly lower bias,  $U = 1.395$  V, the diode emission starts to break up into a series of bright spots dominating over a homogeneous background emission. At  $U = 1.385$  V, the background intensity weakens and several bright spots emerge at distinct positions with a uniform spot size determined by the diameter of the focal spot of the collecting lens. At this voltage the EL spectra fragment into sharp lines. At  $U = 1.372$  V, the number of bright spots decreases and the relative intensities of the individual spots change compared to the image at  $U = 1.385$  V. The spectra now consist of individual emission lines with no background EL. At  $U = 1.345$  V, the maximum intensities are much lower and the number of visible emission spots is reduced to four. At  $U = 1.315$  V, only one bright spot is visible and the corresponding spectrum, shown in Fig. 1d, consists of a single sharp emission line with an intensity similar to the maximum at  $U = 1.372$  V. We note that no other EL lines could be observed at this bias, suggesting that this emission center originates from a single QD.

The EL spectra corresponding to the spatial EL maps are presented in Fig. 3 for  $U = 1.372$  V. Figure 3a shows maps of the normalized EL intensity as a function of position at specific photon energies. The individual scans are distinguished by different colors and the corresponding energies are indicated by arrows in the  $\mu$ EL spectra of Fig. 3b. The bright spots in Fig. 3a and the corresponding EL spectra of Fig. 3b are labeled as P1-P7. Each

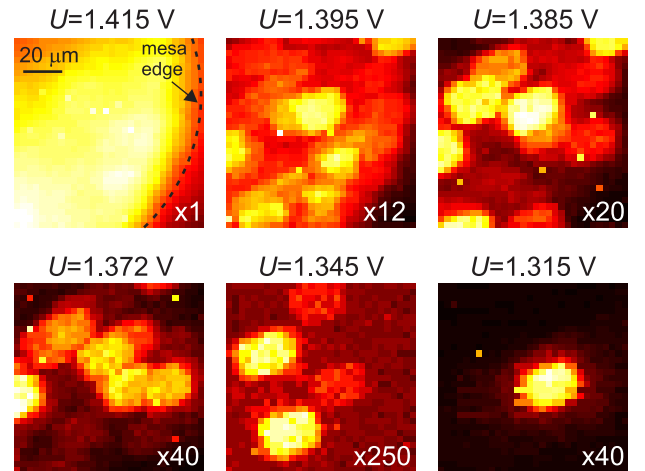


FIG. 2: (Color online) Maps of the maximum surface  $\mu$ EL intensity for a range of applied biases. For a given bias the EL spectrum is recorded for a grid of positions. The images show the maximum intensity of each spectrum as a function of the position on the diode. The number at the bottom right of each image denotes the factor by which the EL intensity is scaled compared to the first image.

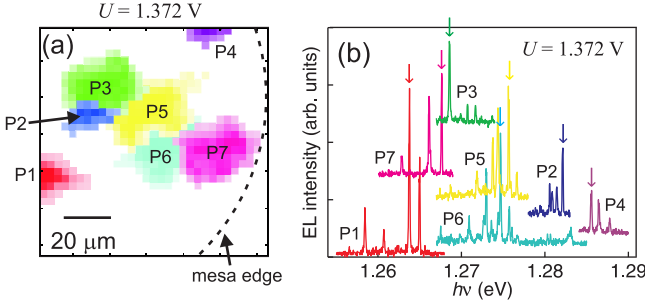


FIG. 3: (Color online) (a) Overlay image of several  $\mu$ EL intensity maps at different photon energies, given by arrows of the same color in (b). The symbols P1-P7 mark the position of the maximum EL intensity at this energy. Features with intensities below the threshold of 10% of the maximum in a scan are omitted for clarity. (b) EL spectra recorded for  $U = 1.372$  V at the positions P1-P7 given in (a). The EL spectra are offset for clarity.

spot has approximately the same size and circular shape as the one that gives rise to the sharp EL emission in Fig. 1d and has a unique spectral fingerprint consisting of a small number of sharp lines. In turn, each emission line originates from exactly one bright spot in the spatial scans [21]. These observations are consistent with the selective excitation of a small number of dots by carriers tunneling in the diode area of the bright spots.

Figure 4a shows the bias dependence of the peak intensity of the emission line L1 of Fig. 1d at the energy  $h\nu = 1.2730$  eV. The EL intensity exhibits sharp peaks at bias voltages of  $U = 1.32$  V and  $U = 1.37$  V. These resonances are a clear manifestation of the voltage-tunable resonant tunneling excitation of a single QD detected by optical means. The resonant injection of carriers from the doped contact layers into discrete excited states of the QD is followed by energy relaxation of the carriers into the ground state and radiative recombination. The two bias resonances are separated in energy by  $\sim 56$  meV and the differences from the ground state are 42 meV and 99 meV, both typical values for the quantum confinement energies of self-assembled InAs QDs. At large biases ( $U > 1.4$  V) the strong growth of the EL intensity arises from an increasing contribution of the emission from the QD ensemble, which is excited through carrier injection and redistribution into the extended states of the wetting layer and of the GaAs matrix as the flat band condition is approached [22]. We find resonances on many other EL lines in this spectral range, though the number of observed resonances and their amplitudes can differ, as shown for the lines L4 and L5 in Fig. 4a.

The emission energy of individual EL lines depends on the applied bias, as can be seen in Fig. 4b, where the energy shift  $\Delta E$  relative to the value at  $U = 1.41$  V is plotted for several lines L1-L5. We attribute this bias dependence to the quantum-confined Stark effect in the

QD [23, 24]. Of particular interest is that the energies of some of the lines remain constant over certain bias ranges. For example, the L1 line does not shift between  $\sim 1.36$  V and 1.38 V, suggesting that the electric field in the intrinsic region remains constant. We propose that resonant tunneling gives rise to an increase in the average charge density in the QD layer, thus screening the local electric field, an effect analogous to the charge build-up effect reported previously for resonant tunneling quantum well diodes [25]. Also note that, although the Stark shifts for various EL lines differ from each other, the rates of shift with bias are very similar. This indicates that the different bias dependences arise from mesoscopic variations of the potential landscape rather than from differences in the electronic properties of the QDs.

Our data demonstrate that at low temperatures the QD EL below the flat band condition is excited by resonant tunneling injection of carriers. The electrons and holes in the doped  $n$ - and  $p$ -type layers adjacent to the  $i$ -region of the diode have an energy spread given by the respective Fermi energies ( $< 10$  meV). Since both the electron and hole states have to be aligned with the Fermi seas to resonantly excite EL, one would expect considerably narrower bias resonances than the ones reported here. On the other hand, the Coulomb interaction of a charged QD with the Fermi seas of the contacts and with its nearest neighbor QDs can provide additional tunneling pathways, thus accounting for the relatively large widths ( $> 10$  mV) of the resonances in Fig. 4a. We note that this broadening is significantly larger than the width of individual QD EL lines ( $\sim 150$   $\mu$ eV).

Though the number of active QDs is constrained by the conditions of resonant tunneling, this constraint is not sufficient to explain the pronounced spectral and spatial fragmentation of the EL emission revealed in our study. Existing theoretical models [16] do not predict such an effect either. The high density and uniform distribution of QDs ensures that even at the lowest bias several dots could be active. Hence we conclude that some QDs are coupled more strongly to the reservoirs than others,

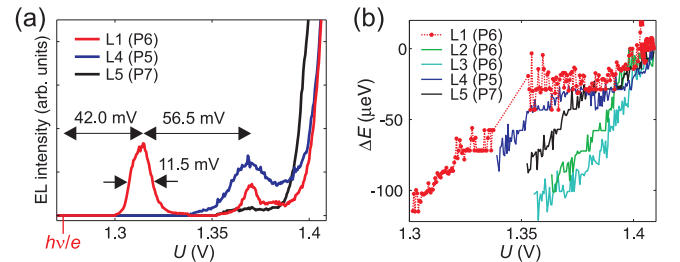


FIG. 4: (Color online) (a) Peak intensity of the L1-L4-L5 lines as a function of bias. The arrows show the energy separation of two resonances from the energy of the L1 line. (b) Energy shift of several EL lines as a function of the bias. P5, P6 and P7 correspond to the positions on the mesa given in Fig. 3a.

which is supported by the different number of observable resonances for different QDs shown in Fig. 4a. Since the emission energies of the investigated QDs are very similar, this variation of the coupling is likely to be due to local variations of the tunnel distance and barrier height. In previous studies,  $\mu$ EL maps of the emission from the ridge-waveguide regions of InGaN quantum well based LEDs have revealed spatial inhomogeneities due to non-uniform carrier injection caused by crystal degradation [26]. In our diodes, the EL spectra are stable with time, but preferential tunneling paths may arise from mesoscopic fluctuations of the  $n$ - and  $p$ -doped interfaces due to randomly placed dopant atoms in or close to the intrinsic region, crystals defects or strain-related potential minima associated with the QDs themselves. Such variations would not only explain the spatial and spectral fragmentation of the EL spectra, but could also account for some differences in the bias dependence of the Stark shifts among various QDs.

In summary, we have demonstrated how the homogeneous broad band emission of a large quantum dot ensemble fragments into spatially strongly inhomogeneous sharp emission lines from individual quantum dots. Each EL line exhibits a distinct resonance behavior as a function of the applied bias and a unique Stark shift. These effects can be explained in terms of the selective excitation of a small number of QDs within the ensemble due to the presence of preferential resonant tunneling paths for carriers. Our results provide direct evidence for the resonant and voltage tunable electrical injection of carriers into individual QDs and are relevant for future implementation of such structures into electrically controlled single photon LEDs. In particular, the resonant tunneling excitation of a single dot could reduce quantum decoherence due to interactions with carriers occupying adjacent dots or higher energy continuum states.

## ACKNOWLEDGEMENTS

This work is supported by the Engineering and Physical Sciences Research Council (UK) and the Deutsche Forschungsgemeinschaft in the frame of SFB 787.

---

\* Electronic address: andreas.baumgartner@unibas.ch

† present address: Nanoelectronics Group, University of Basel, Switzerland

- [1] A.D. Yoffe, *Advances in Physics* **50**, 1 (2001).
- [2] D. Bimberg, *Electron. Lett.* **44**, 3 (2008).
- [3] N.N. Ledentsov, D. Bimberg, and Zh.I. Alferov, *J. Light-wave Technol.* **26**, 1540 (2008).
- [4] J.-Y. Marzin, J.-M. Gerard, A. Izrael, D. Barrier, and G. Bastard, *Phys. Rev. Lett.* **73**, 716 (1994).
- [5] Z. Yuan, B.E. Kardynal, R.M. Stevenson, A.J. Shields, C.J. Lobo, K. Cooper, N.S. Beattie, D.A. Ritchie, and M. Pepper, *Science* **295**, 102 (2002).
- [6] P. Michler, A. Kiraz, C. Becher, W.V. Schoenfeld, P.M. Petroff, L. Zhang, E. Hu, and A. Imamoglu, *Science* **290**, 2282 (2000).
- [7] M. Nomura, N. Kumagai, S. Iwamoto, Y. Ota, and Y. Arakawa, *Nat. Phys.* **6**, 279 (2010).
- [8] N. Panev, A.I. Persson, N. Sköld, and L. Samuelson, *Appl. Phys. Lett.* **83**, 2238 (2003).
- [9] J. Claudon, J. Bleuse, N.S. Malik, M. Bazin, P. Jaffrennou, N. Gregersen, C. Sauvan, P. Lalanne, and J.-M. Gérard, *Nat. Photonics* **4**, 174 (2010).
- [10] R.M. Stevenson, R.J. Young, P. Atkinson, K. Cooper, D.A. Ritchie, and A.J. Shields, *Nature* **439**, 179 (2006).
- [11] C.L. Salter, R.M. Stevenson, I. Farrer, C.A. Nicoll, D.A. Ritchie, and A.J. Shields, *Nature* **465**, 594 (2010).
- [12] M. Narihiro, G. Yusa, Y. Nakamura, T. Noda, and H. Sakaki, *Appl. Phys. Lett.* **70**, 105 (1997).
- [13] I. Hapke-Wurst, U. Zeitler, H. Frahm, A.G.M. Jansen, R.J. Haug, and K. Pierz, *Phys. Rev. B* **62**, 12621 (2000).
- [14] A. Patané, R.J.A. Hill, L. Eaves, P.C. Main, M. Henini, M.L. Zambrano, A. Levin, N. Mori, C. Hamaguchi, Yu.V. Dubrovskii, E.E. Vdovin, D.G. Austing, S. Tarucha, and G. Hill, *Phys. Rev. B* **65**, 165308 (2002).
- [15] D. Reuter, P. Kailuweit, A.D. Wieck, U. Zeitler, O. Wibbelhoff, C. Meier, A. Lorke, and J.C. Maan, *Phys. Rev. Lett.* **94**, 026808 (2005).
- [16] G. Kiesslich, A. Wacker, E. Schöll, S.A. Vitusevich, A.E. Belyaev, S.V. Danylyuk, A. Förster, N. Klein, and M. Henini, *Phys. Rev. B* **68**, 125331 (2003).
- [17] L. Turyanska, A. Baumgartner, A. Chaggar, A. Patané, L. Eaves, and M. Henini, *Appl. Phys. Lett.* **89**, 092106 (2006).
- [18] G. Ortner, D.R. Yakovlev, M. Bayer, S. Rudin, T.L. Reinecke, S. Fafard, Z. Wasilewski, and A. Forchel, *Phys. Rev. B* **70**, 201301(R) (2004).
- [19] E. Stock, A. Baumgartner, M. Dachner, T. Warming, A. Schliwa, A. Patané, L. Eaves, M. Richter, A. Knorr, M. Henini, and D. Bimberg, *Conference on Lasers and Electro-Optics, and Quantum Electronics and Laser Science Conference (CLEO/QELS 2009)* **1-5**, 2418 (2009).
- [20] The large scale deviations in the image are mainly due to a misalignment of the focal plane of the lens and the sample surface.
- [21] A small number of weak emission lines occur in more than one spectrum due to stray light from overlapping collection areas.
- [22] A. Baumgartner, A. Chaggar, A. Patané, L. Eaves, and M. Henini, *Appl. Phys. Lett.* **92**, 091121 (2008).
- [23] P.W. Fry, I.E. Itskevich, D.J. Mowbray, M.S. Skolnick, J.J. Finley, J.A. Barker, E.P. O'Reilly, L.R. Wilson, I.A. Larkin, P.A. Maksym, M. Hopkinson, M. Al-Khafaji, J.P.R. David, A.G. Cullis, G. Hill, and J.C. Clark, *Phys. Rev. Lett.* **84**, 733 (2000).
- [24] A. Patané, A. Levin, A. Polimeni, F. Schindler, P.C. Main, L. Eaves, and M. Henini, *Appl. Phys. Lett.* **77**, 2979 (2000).
- [25] M.L. Leadbeater, E.S. Alves, F.W. Sheard, L. Eaves, M. Henini, O.H. Hughes, and G.A. Toombs, *J. Phys. Condens. Matter* **1**, 10605 (1989).
- [26] M. Rossetti, T.M. Smeeton, W.-S. Tan, M. Kauer, S.E. Hooper, J. Heffernan, H. Xiu, and C.J. Humphreys, *Appl. Phys. Lett.* **92**, 151110 (2008).